Title: Paleoenvironmental conditions, source and maturation of Neogene organic matter from the siliciclastic deposits of the Orava-Nowy Targ Basin

Author: Elżbieta Jaroszewicz, Maciej Bojanowski, Leszek Marynowski, Maciej Łoziński, Anna Wysocka

Citation style: Jaroszewicz Elżbieta, Bojanowski Maciej, Marynowski Leszek, Łoziński Maciej, Wysocka Anna. (2018). Paleoenvironmental conditions, source and maturation of Neogene organic matter from the siliciclastic deposits of the Orava-Nowy Targ Basin. "International Journal of Coal Geology" (Vol. 196 (2018), s. 288-301), doi 10.1016/j.coal.2018.07.016

International Journal of Coal Geology 196 (2018) 288–301

Contents lists available at ScienceDirect

International Journal of Coal Geology

journal homepage: www.elsevier.com/locate/coal

Paleoenvironmental conditions, source and maturation of Neogene organic matter from the siliciclastic deposits of the Orava-Nowy Targ Basin

Elżbieta Jaroszewicz[a,*], Maciej Bojanowski[a], Leszek Marynowski[b], Maciej Łoziński[c], Anna Wysocka[c]

[a] Institute of Geological Sciences, Polish Academy of Sciences, Twarda 51/55, 00-818 Warsaw, Poland
[b] Faculty of Earth Sciences, University of Silesia, Będzińska 60, 41-200 Sosnowiec, Poland
[c] Faculty of Geology, University of Warsaw, Żwirki i Wigury 93, 02-089 Warsaw, Poland

ARTICLE INFO

Keywords:
Orava-Nowy Targ Basin
Neogene lignites
Biomarkers
Thermal maturity
Paleoenvironment

ABSTRACT

The Orava-Nowy Targ Basin (ONTB) is an intramontane depression filled with Neogene and Quaternary deposits located at the junction of the Inner and Outer Carpathians. The Neogene infill of the basin consists mainly of siliciclastic rocks with very common lignite intercalations and is mostly of fluvial or lake origin.

The organic matter molecular analysis of seventeen Neogene samples confirmed the terrigenous origin of organic matter with a predominance of higher plant input in most samples, based on the distribution of *n*-alkanes and steranes, as well as the presence of tri- and tetracyclic diterpenoids, and triterpenoids representing oleanane, ursane, lupane, chrysene and picene derivatives. High concentrations of compounds originating from both angiosperms and gymnosperms suggest the presence of mixed forests. Additionally, important input of mosses into the primary organic matter is indicated by the high concentration of *n*-C_{23} and presence of hop-17(21)-enes in most samples. A high Average Aromatic Ring and Conifer Wood Degradation Index > 0.7 indicate high activity of bacteria and wood-degrading fungi in the sedimentary environment. There was no evidence of weathering and scarce signs of biodegradation were identified. All samples were subjected to water washing.

Huminite reflectance and biomarker-based parameters, as well as the presence of unsaturated pentacyclic triterpenoids and steroids indicate an immature organic matter. A trend of decreasing maturation of sediments from east to the west was observed, as was a similarity of thermal maturity between the Podhale Synclinorium and the ONTB, although the latter seems to be coincidental. A thermal gradient value of 35 °C/km was assumed for calculating the maximum thickness of eroded strata, resulting in 1–1.6 km for the SE area and a maximum temperature of the deepest buried samples equal to 45–65 °C.

1. Introduction

The Orava-Nowy Targ Basin (ONTB) is in the Slovak-Polish cross-border area in the Western Carpathians. It constitutes an intramontane depression, which developed in a fully continental setting upon bedrock composed of three different, older structural units (Fig. 1). The Neogene infill of the basin consists mainly of fine-grained siliciclastics that were deposited in fluvial and lake environments (e.g., Łoziński et al., 2015). Paleoenvironmental reconstruction of the basin is hindered by the scarcity of fauna in these facies. Furthermore, the domination of siliciclastic facies precludes the application of inorganic geochemical analyses as paleoenvironmental proxies. Therefore, organic matter appears to be a potentially valuable source of information in this regard, especially as the basin has not been deeply buried. The Neogene siliciclastic deposits exhibit variable contents of organic matter and are intercalated with thin lignite seams, making them suitable for organic geochemical investigation. Thus, the principal goal of this work was to characterize the paleoenvironmental conditions and the source of organic matter through biomarker analysis.

Organic matter is frequently used for the reconstruction of the thermal and burial histories. One of the older units underlying the ONTB is the Podhale Synclinorium (PS) (Fig. 1), where systematic studies of thermal maturity were completed by Wagner (2011), Marynowski et al. (2006) and Środoń et al. (2006) using vitrinite reflectance, biomarkers and illite/smectite measurements, respectively. The above methods revealed a clear trend in the thermal maturity

* Corresponding author.
E-mail addresses: e.jaroszewicz@twarda.pan.pl (E. Jaroszewicz), mbojan@twarda.pan.pl (M. Bojanowski), leszek.marynowski@us.edu.pl (L. Marynowski), maciej.lozinski@uw.edu.pl (M. Łoziński), Anna.Wysocka@uw.edu.pl (A. Wysocka).

https://doi.org/10.1016/j.coal.2018.07.016
Received 8 May 2018; Received in revised form 25 July 2018; Accepted 31 July 2018
Available online 01 August 2018

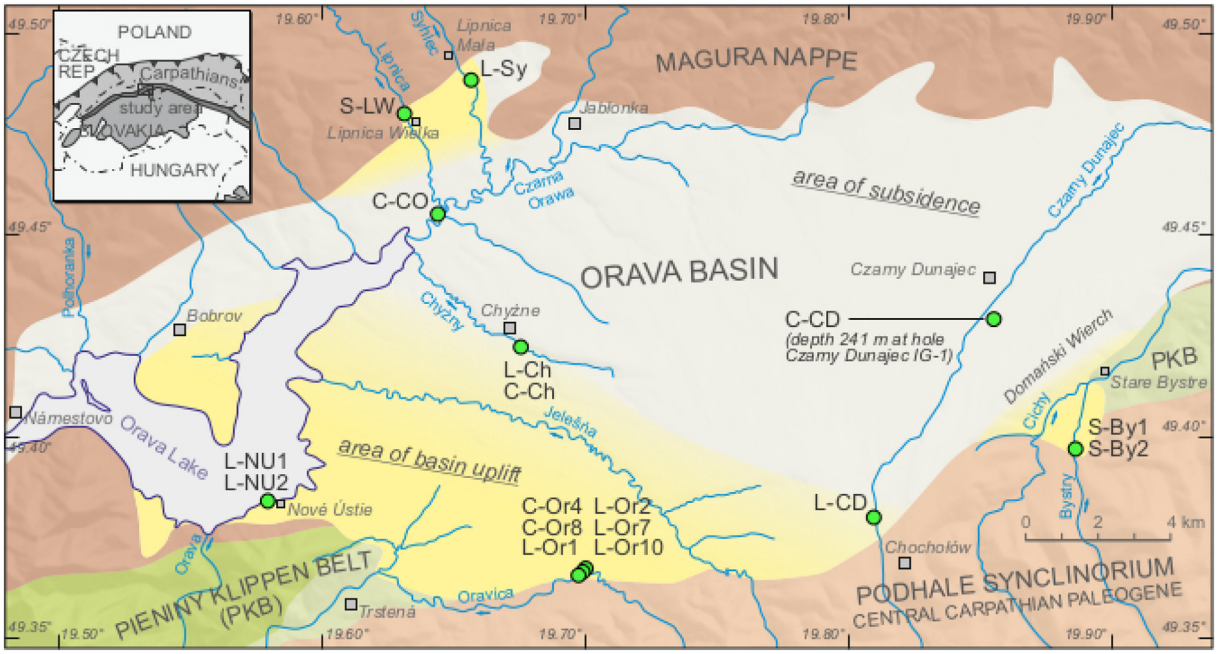

Fig. 1. Schematic map of the ONTB with marked sample locations. Areas of basin uplift are shown in yellow (after Łoziński et al., 2017; modified). (For interpretation of the references to colour in this figure legend, the reader is referred to the web version of this article.)

across this unit, which was related to the tectonically controlled differential exhumation of the PS. We applied biomarker-based indices of thermal maturity and measured the vitrinite reflectance in the ONTB, then compared these results with those for the PS to estimate the magnitude and timing of the exhumation in the region. Moreover, we evaluated the applicability of different biomarker-based thermal maturity indices for terrestrial organic matter dominated by a higher plant source with low maturity and not obliterated by weathering, although influenced by water washing.

2. Geological setting

The Orava-Nowy Targ Basin (ONTB) is in the Polish–Slovak cross border area north and north-west from the strongly elevated Tatra Mountains (Fig. 1). The ONTB is an E-W stretching intramontane basin, which can be divided into two parts – eastern (Nowy Targ) and western (Orava). The basin infill consists of terrigenous Neogene and Quaternary strata, which overlays partially eroded older units (e.g., Watycha, 1976) (Fig. 1): Podhale Synclinorium (PS), consisting of Lutetian-Bartonian to Egerian rocks of the Central Carpathian Paleogene Basin (Sotak, 1998a, 1998b; Garecka, 2005); Pieniny Klippen Belt (PKB), consisting of strongly tectonized Early Jurassic – Paleogene rocks (e.g., Birkenmajer, 1960); and Magura Nappe, consisting of Albian/Cenomanian – Early Miocene rocks (e.g., Birkenmajer and Oszczypko, 1989; Cieszkowski et al., 1989).

The base of the ONTB undulates and attains two depth maxima: 150 m near Nowy Targ and above 1000 m in Orava, and these are separated by the elevation between Ludźmierz and Rogoźnik (Watycha, 1976). Neogene deposits in Orava consist of a series of clastic sediments – gravels, sandstones, siltstones and claystones with common lignite lenses and intercalations. The strata generally lay subhorizontally, although at the basin margin, the dips of the strata increase up to 20–25° towards the basin center. These clastic sediments were predominantly transported by streams and rivers from the mountains surrounding the basin. They were arranged in alluvial fans propagating towards the center of the basin, where freshwater lakes and swamps developed (Watycha, 1976; Łoziński et al., 2015). Freshwater fauna, mainly snails, are rather infrequent in these deposits. Consequently, the age of sedimentation onset is still discussed and has been estimated to be Late Oligocene/Early Miocene (Watycha, 1976), Badenian (Oszast and Stuchlik, 1977) or Sarmatian (Nagy et al., 1996; Wysocka et al., 2018). Provenance studies of the basin infill revealed that detrital material was derived mainly from the Podhale and Magura Units. Lithoclasts from the PKB are also common in places, but material eroded from the Tatra Mountains is found only in the Quaternary deposits (Watycha, 1976; Tokarski et al., 2012).

Previous paleoenvironmental studies of the ONTB Neogene infill are especially important for this work. Oszast and Stuchlik (1977) have shown that the main type of plant communities present in the examined area during the Neogene was forest, which differed depending on water availability in different parts of the ONTB. Swamps were covered with swamp forests with *Cupressaceae-Taxodiaceae* trees or swamp thickets with *Betulaceae-Myricaceae-Cyrillaceae* and herbaceous plants. Forests with alder, willow, poplar, platanus and pterocarya trees have also been identified. The slopes of the mountains surrounding the basin were overgrown by mixed forests with a predominance of broad-leaved trees.

The presence of such plant communities allowed the formation of lignites. Lignites are up to 2 m thick, and their lateral extent is relatively small, but they are very common in the studied sediments, especially in the Miocene strata. They exhibit a relatively high abundance of cutinite and a high degree of gelification (Nagy et al., 1996). Their origin has been interpreted as both autochthonous, from local swamps and shallow lakes, and allochthonous, from the fragments of trees brought into the basin by rivers and streams (Nagy et al., 1996).

Sedimentation in the Magura Unit and Podhale Basin halted in the Early Miocene and was followed by the uplift and folding of the sediments. Thrusting of the Magura Unit started in the north, and the deformation front migrated towards the south. At the transition from the Early to Middle Miocene, the PS was already folded, and tectonic contacts between all three units underlying the ONTB were formed (e.g., Watycha, 1976). The sedimentation in the ONTB started on the erosional surface of the PS, PKB and Magura Unit (Oszast and Stuchlik, 1977). The origin of the ONTB has been widely discussed in the literature, but most authors suggest that it must have been related to a strike-slip mechanism (Baumgart-Kotarba, 1996; Tokarski et al., 2012). The regional fault systems started to form during the Late Oligocene-

Table 1
Samples' bulk characteristics and fractional compositions.

Sample	TOC [%]	TS [%]	EOM [mg/g rock]	Aliphatic fraction [% EOM]	Aromatic fraction [% EOM]	Polar fraction [% EOM]
L-Or7	48.15	1.24	17.57	4.65	2.33	93.02
L-Or1	31.04	4.06	20.85	1.36	1.36	97.28
L-Or2	53.49	3.77	16.07	4.52	1.56	93.92
L-Or10	52.96	3.87	13.40	1.37	1.37	97.26
L-Sy	56.88	0.77	14.30	5.61	2.68	91.71
L-Ch	51.58	3.97	27.67	1.27	2.53	96.20
L-CD	53.26	1.73	16.63	1.51	3.24	95.25
L-NU1	43.06	8.79	8.90	4.57	1.81	93.62
L-NU2	52.40	4.96	12.02	3.44	4.16	92.40
C-Or4	0.24	0.01	0.21	33.33	33.33	33.33
C-Or8	7.91	3.12	2.58	5.62	1.12	93.26
C-Ch	0.30	0.02	0.26	7.14	7.14	85.71
C-CO	–	–	–	11.76	5.88	82.35
C-CD	15.38	1.31	6.99	1.28	1.80	96.92
S-By1	1.79	0.05	0.63	7.89	5.26	86.84
S-By2	2.77	0.11	1.31	5.08	3.39	91.53
S-LW	2.36	0.09	0.88	2.50	2.50	95.00

TOC = Total Organic Carbon
TS = Total Sulfur
EOM = Extractable Organic Matter

Miocene in the Western Carpathians (Kováč and Hók, 1993; Kováč et al., 1998). One of the main strike-slip movements started during the Eggenburgian in the Vienna Basin and propagated towards the north-east, most likely leading to the formation of the ONTB (e.g., Tokarski et al., 2012). Sedimentation in the ONTB likely began around Badenian-Sarmatian, but an exact age is difficult to estimate, as there is no agreement on the age of the onset of sedimentation (Oszast and Stuchlik, 1977; Baumgart-Kotarba, 1996; Nagy et al., 1996; Wysocka et al., 2018). Subsidence ceased in the Pliocene and was followed by a partial uplift during the Late Pliocene, which persists (Vanko, 1988; Nagy et al., 1996; Baumgart-Kotarba, 2001; Tokarski et al., 2012; Łoziński et al., 2017).

3. Material and methods

Seventeen samples of Neogene deposits from different locations were chosen for geochemical studies (Fig. 1). Nine lignite samples (marked with a "L" prefix) were collected from the well-exposed strata at the banks of the Oravica River near Čimhova (L-Or7, L-Or1, L-Or2, L-Or10), the Syhlec Stream near Lipnica Mała (L-Sy), the Chyżny Stream near Chyżne (L-Ch), the Czarny Dunajec River near Chochołów (L-CD) and from the southern shore of Orava Lake near Nove Ústie (L-NU1 and L-NU2). Five claystone samples (marked with a "C" prefix) were obtained from outcrops at the banks of the Oravica River near Čimhova (C-Or4, C-Or8), a stream near Chyżne (C-Ch), the Czarna Orawa River (C-CO) and from the Czarny Dunajec IG-1 borehole (C-CD; depth 240.6–241.6). Three siltstone samples (marked with a "S" prefix) were collected from the Bystry Stream bank near Miętustwo (S-By1, S-By2) and from a small stream bank near Lipnica Wielka (S-LW). The material was collected from deposits of marshy and swampy areas (lignites and claystones), as well as from extensive floodplains with small flow channels and ephemeral ponds (sandstones, siltstones and claystones). The Nove Ústie, Oravica River, Czarny Dunajec River and Bystry Stream sections are located along the southern margin and close to the base of the ONTB, and the collected samples represent the same basal interval of the basin infill.

Total organic carbon (TOC) and total sulfur (TS) contents were determined for all the samples, except for sample C-CO, using an ELTRA CS-530 analyzer. Vitrinite reflectance (R_o) was determined using an Axio Imager M2M in three lignite samples (L-CD, L-Or1 and L-Or2). One-hundred measurements were performed for each sample. All seventeen samples were crushed and powdered. Extraction of bitumens was performed in a Soxhlet apparatus for 72 h with a dichloromethane/methanol (93/7, v/v) mixture. To separate extracts into aliphatic, aromatic and polar fractions, modified column chromatography was used (Bastow et al., 2007). Samples were placed at the top of a Pasteur pipette filled with silica gel which had been activated for 8 h at 110 °C. Hydrocarbon aliphatic, aromatic and polar fractions were eluted under gravity with 2 ml of an *n*-pentane, *n*-pentane/dichloromethane (7/3) mixture and a dichloromethane/methanol (1/1) mixture, respectively. Aliquots of the polar fractions were converted to trimethylsilyl (TMS) derivatives by reaction with *N,O*-bis-(trimethylsilyl)trifluoroacetamide (BSTFA), 1% trimethylchlorosilane, and pyridine for 3 h at 70 °C.

GC-MS analyses were performed on aliphatic and aromatic fractions with an Agilent Technologies 6890 series II gas chromatograph (GC) and an Agilent 5973 Network mass spectrometer (MS). Helium was used as a carrier gas (flow rate of 1 ml/min). A J&W DB35-MS capillary column (60 m, 0.25 mm i.d., 0.25 μm film thickness) coated with a chemically bonded phase (35% polymethylsiloxane 65% diphenylsiloxane) was used. A GC oven was preheated to 50 °C, which was held constant for 1 min and then heated to 120 °C at a 20 °C/min rate and to 300 °C at a 3 °C/min rate. The column was then held isothermal for 50 min. The GC column outlet was connected directly to the ion source of the mass spectrometer. Mass spectra were recorded from *m/z* 45–550 (0–40 min) and *m/z* 50–700 (above 40 min). The MS was operated in electron impact mode (ionization energy 70 eV). Individual compounds were identified based on retention time and mass spectra in comparison with previously published data. Extraction and separation were carried out at the Faculty of Geology, University of Warsaw, Poland, while the instrumental analyses (TOC, TS, R_o, GC–MS) were completed at the Faculty of Earth Sciences, University of Silesia, Poland.

4. Results

4.1. Bulk organic geochemistry

Total organic carbon (TOC) content ranges from 0.2% to 15.4% in clastic samples and from 31.0% to 56.9% in lignites (Table 1). Total sulfur (TS) content is rather low in the clastic samples (< 0.5%) (Table 1). Only two claystones (C-Or8 and C-CD) show elevated sulfur content (3.1% and 1.3%, respectively). TS in lignites ranges from 0.8% to 8.8%. Lignite samples can be divided into two populations: samples with relatively low (< 2%) TS values (L-CD, L-Sy and L-Or7) and samples with higher sulfur content (> 3.5%; L-Or1, L-Or2, L-Or10, L-Ch, L-NU1 and L-NU2) (Table 1). Extractable organic matter (EOM) content ranges from 0.21 to 27.67 mg/g of rock with lignites showing considerably higher values than clastic rocks (Table 1). The polar fraction is dominant in almost all samples, ranging from 82.3% (C-CO) to 97.3% (L-Or1) (Table 1). Aliphatic and aromatic fraction contents range from 1.3% (L-Ch) to 11.8% (C-CO) and from 1.1% (sample C-Or8) to 5.9% (sample C-CO), respectively (Table 1). Sample C-Or4 is an exception with equal amounts of all three hydrocarbon fractions. This pattern is likely related to an extremely small amount of EOM in this sample. Unresolved complex mixture (UCM) (Milner et al., 1977; Rubinstein et al., 1977; Killops and Al-Juboori, 1990; Peters et al., 2005a) is present in sample C-CO. It is also noticeable in sample C-Or4, although not as significant as in the former sample.

4.2. n-Alkanes and acyclic isoprenoids

The distribution of *n*-alkanes in the samples studied is usually in the range from *n*-C_{16} to *n*-C_{35} (Figs. 2 and 3). Most samples show a unimodal distribution with notable odd-over-even predominance and a maximum at *n*-C_{29} or *n*-C_{31}. One sample (C-Or8) has a unimodal distribution with a maximum at *n*-C_{23} (Fig. 2). Other samples (S-By2, L-Or2 and L-NU1) are characterized by odd-over-even predominance and a bimodal distribution, with the first maximum at *n*-C_{23} and the second

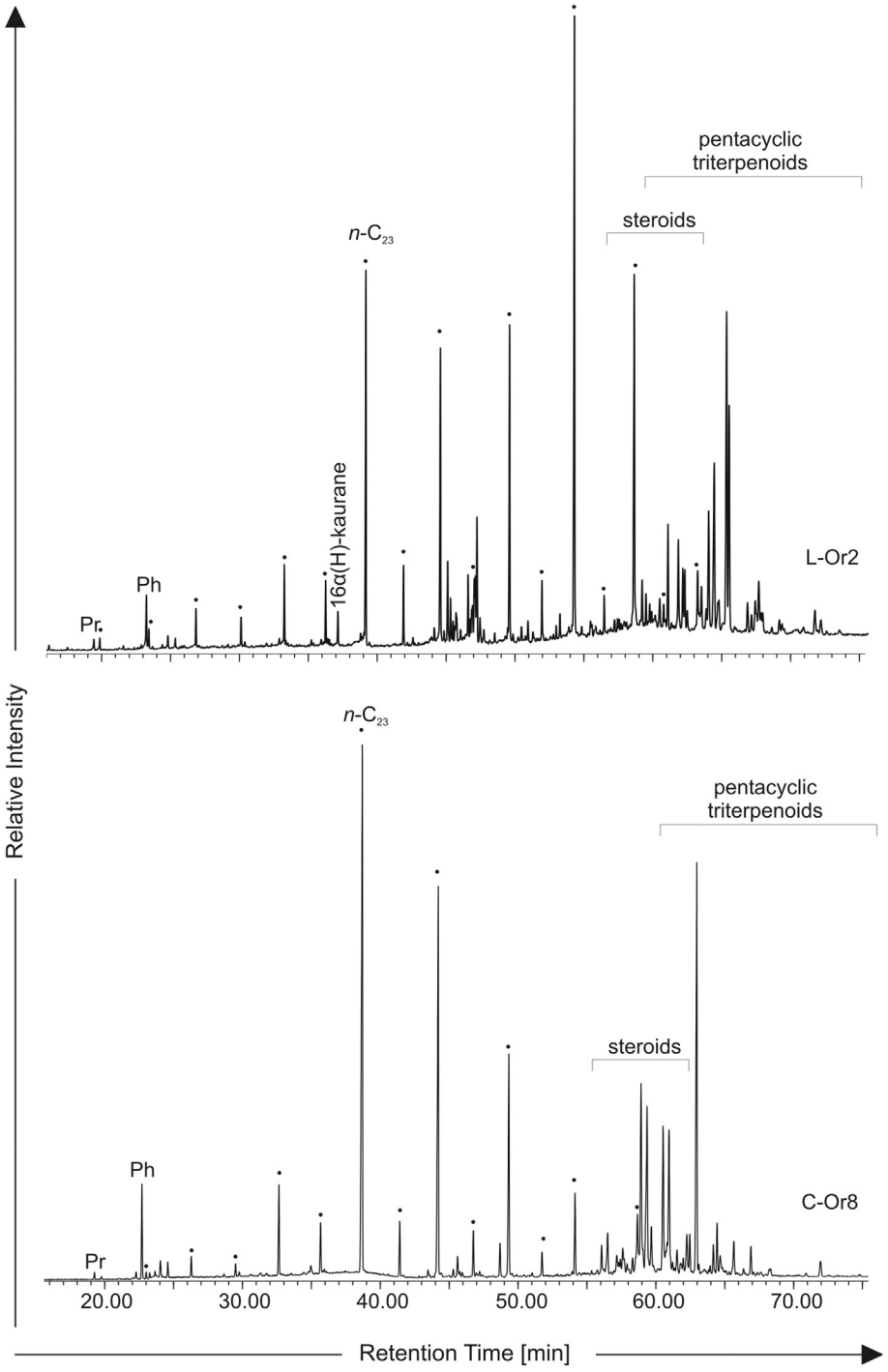

Fig. 2. Total Ion Current (TIC) of the aliphatic fractions (samples L-Or2 and C-Or8). *n*-Alkanes are marked by dots.

at *n*-C_{31}, *n*-C_{29} and *n*-C_{27}, respectively (Figs. 2 and 3).

Samples C-CO and L-Sy (Fig. 3) show slightly different characteristics. The distribution of *n*-alkanes is bimodal with maxima at *n*-C_{22} and *n*-C_{29}. In the range between *n*-C_{17} and *n*-C_{23}, a slight even-over-odd predominance can be observed, while among the long-chain *n*-alkanes, a significant odd-over-even tendency is present. Moreover, the distribution of *n*-alkanes in all the samples show a specific "cut" shape of chromatogram in the range of short-chain compounds.

The Carbon Preference Index (CPI) provides information about the origin and thermal maturity of organic matter (Killops and Killops, 2005; Peters et al., 2005a). CPI values were calculated according to the following formula: $0.5[\Sigma(n\text{-}C_{25}\text{-}n\text{-}C_{33})_{odd} + \Sigma(n\text{-}C_{23}\text{-}n\text{-}C_{31})_{odd}]/\ \Sigma(n\text{-}C_{24}\text{-}n\text{-}C_{32})_{even}]$ (Bray and Evans, 1961). CPI values vary from 1.53 to 8.41 (Table 2), which indicates terrigenous and immature organic matter (Bray and Evans, 1961; Scalan and Smith, 1970; Peters et al., 2005b). The ratio of short-chain to long-chain *n*-alkanes, SCh/LCh = (*n*-C_{17}-*n*-C_{19})/(*n*-C_{27}-*n*-C_{29}), also helps to determine the source of organic matter (Tissot and Welte, 1984; Bourbonniere and Meyers, 1996; Killops and Killops, 2005; Peters et al., 2005b). The SCh/LCh values range from 0.01 to 0.32 (Table 2).

The Alkane Index, AI = *n*-C_{31}/(*n*-C_{31} + *n*-C_{29}), is higher than 0.5 in only three samples (C-Or4, S-By1 and S-By2) (Table 2), which suggests that grasses were the main type of vegetation. Other samples show values lower than 0.5, which indicates trees as the main source of

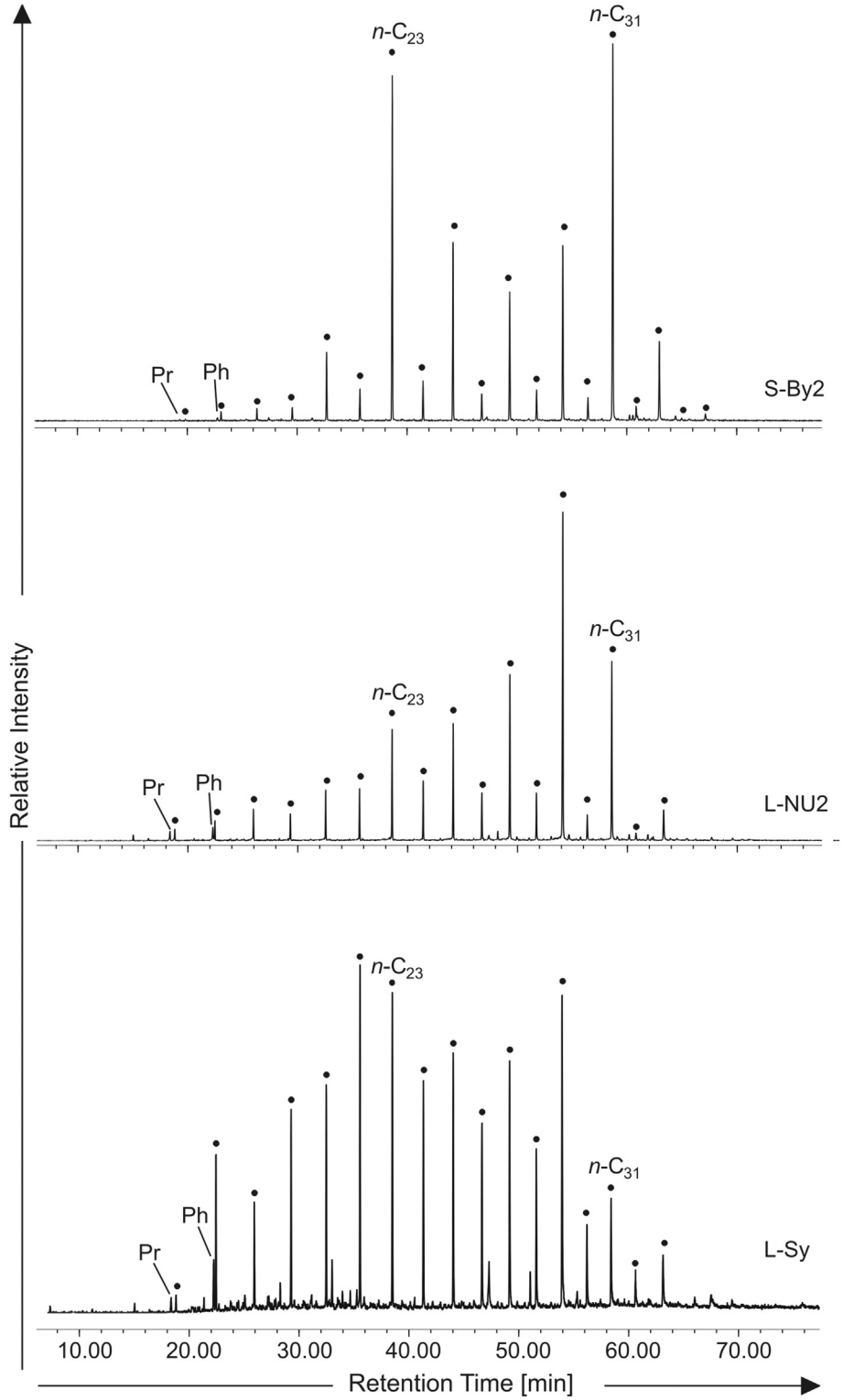

Fig. 3. Gas chromatograms (m/z = 71) of the *n*-alkanes distribution of the samples S-By2, L-NU2 and L-Sy. *n*-Alkanes are marked by dots, Pr – pristane, Ph – phytane.

organic matter (Schefuss et al., 2003; Zhang et al., 2006). Generally, most samples from Oravica exhibit lower values than other samples, while lignites have slightly lower values than the clastic rocks. Worth mentioning is also the relatively high abundance of n-C_{23} in many samples (Figs. 2 and 3). A n-C_{23}/n-C_{31} ratio higher than 0.35 indicates a significant input of *Sphagnum* organic matter (Pancost et al., 2002) in many samples, especially in L-Or2, L-NU1, S-By2 and C-Or8, with the maximum value of 16.37 in sample C-Or8 (Table 2).

Pristane and phytane are acyclic isoprenoids that may originate from chlorophyll or from cell membranes of archaeons, zooplankton, plants or algae (Goossens et al., 1984; Ten Haven et al., 1987; Peters et al., 2005b). These compounds are present in most samples, but their concentrations are low. The pristane to phytane (Pr/Ph) ratio may provide information about the redox conditions of the sedimentary environment, if their source is limited to chlorophyll. However, this index should be treated with caution in the case of lignites, as smaller

Table 2
Calculated biomarkers parameters for samples studied.

Sample	CPI	AI	n-C_{23}/n-C_{31}	Pr/Ph	SCh/LCh	C_{30} $\beta\alpha/\alpha\beta$	C_{31} $\beta\beta/(\beta\beta+\alpha\beta+\beta\alpha)$	20S/(20S + 20R)	Steranes/sterenes	Regular steranes/$\alpha\beta$ hopanes
L-Or7	2.05	0.29	1.30	–	0.07	–	–	–	–	–
L-Or1	4.22	0.31	0.32	0.35	0.06	–	0.47	0.26	0.09	0.28
L-Or2	7.28	0.33	1.12	0.22	0.07	–	0.46	0.27	0.11	0.54
L-Or10	4.67	0.25	0.35	0.36	0.04	–	–	–	0.06	0.004
L-Sy	1.53	0.27	2.28	0.26	0.32	–	–	–	–	–
L-Ch	4.95	0.30	0.32	–	0.03	–	0.49	–	–	–
L-CD	4.94	0.33	0.58	0.48	0.13	–	0.28	–	0.05	0.39
L-NU1	6.18	0.39	1.62	0.41	0.06	–	0.51	0.29	0.20	0.63
L-NU2	4.77	0.34	0.52	0.64	0.10	–	0.46	0.34	0.11	0.66
C-Or4	3.53	0.59	0.13	–	–	–	–	–	–	–
C-Or8	8.41	0.35	16.37	0.08	0.09	0.45	0.55	0.22	0.23	0.80
C-Ch	3.24	0.45	0.33	–	0.02	–	–	–	–	–
C-CO	1.74	0.47	0.50	0.92	0.13	–	–	–	–	–
C-CD	5.17	0.38	0.35	0.61	0.11	–	0.35	0.26	0.40	0.33
S-By1	5.65	0.53	0.31	–	0.03	–	0.15	0.17	0.92	0.67
S-By2	8.02	0.68	0.82	0.36	0.06	0.18	0.45	0.15	0.58	0.55
S-LW	7.01	0.37	0.19	–	0.01	0.27	0.34	0.13	0.39	0.96

CPI = Carbon Preference Index: 0,5 [$\Sigma(n\text{-}C_{25}$ - $n\text{-}C_{33})_{odd}$ + $\Sigma(n\text{-}C_{23}$ - $n\text{-}C_{31})_{odd}$]/ $\Sigma(n\text{-}C_{24}$ - $n\text{-}C_{32})_{even}$ (Bray and Evans, 1961)
AI = Alkane Index: $n\text{-}C_{31}/(n\text{-}C_{31}+n\text{-}C_{29})$ (Schefuss et al., 2003)
Pr/Ph = pristane/phytane
SCh/LCh = short-chain to long-chain n-alkanes: $(n\text{-}C_{17}$ - $n\text{-}C_{19})/(n\text{-}C_{27}$ - $n\text{-}C_{29})$ (Tissot and Welte, 1984)
C_{30} $\beta\alpha/\alpha\beta$ = C_{30} moretane/hopane (Mackenzie et al., 1980)
C_{31} $\beta\beta/(\beta\beta+\alpha\beta+\beta\alpha)$ = homohopane C_{31} $\beta\beta/(\beta\beta+\alpha\beta+\beta\alpha)$ (Sinninghe Damstè et al., 1995)
Steranes/sterenes = $\Sigma(C_{27}$-C_{29} steranes)/$\Sigma(C_{27}$-C_{29} sterenes) (Amo et al., 2007)
Regular steranes/ $\alpha\beta$ hopanes = $\Sigma(C_{27}$-C_{29} $\alpha\alpha\alpha$ and $\alpha\beta\beta$, R and S steranes)/$\Sigma(C_{29}$-C_{33} $\alpha\beta$, R and S hopanes) (Tissot and Welte, 1984)

amounts of phytane are usually extracted from the lignite macromolecule to the bituminous fraction due to low maturity (Connan, 1974; Volkman and Maxwell, 1986; Peters et al., 2005b). Nevertheless, phytane predominates over pristane in all the samples, resulting in a Pr/Ph ratio ranging from 0.08 to 0.92 (Table 2).

4.3. Tri- and tetracyclic diterpenoids

Diterpenoids were identified in most samples, although in rather small amounts with the exceptions of samples L-Or10, L-Ch, L-LM and C-CD. The most common tetracyclic diterpenoid is 16α(H)-phyllocladane, and it is the dominant compound from that group in siltstones (Fig. 4). Only in a few samples other diterpenoids, i.e. 16β(H)-phyllocladane, 16α(H)-kaurane and *ent*-beyerane, were identified. Various tricyclic diterpenoid were identified as well; pimarane, isopimarane and abietane were the most abundant (Fig. 4), but norpimarane, rimuene and fichtelite were also present. Although isopimarane was identified only in a few samples, a certain relation was observed, as it was more abundant in the lignites than in clastic rocks.

4.4. Pentacyclic hopanoid triterpenoids

Pentacyclic hopanoid triterpenoids were present in most samples, although in relatively low amounts. Both hopanes and hopenes were identified (Fig. 5). A predominance of C_{30} hop-17(21)-ene over other hopanoids was observed (Fig. 5). Among hopanes, C_{29} to C_{32} compounds with configurations of $\alpha\beta$, $\beta\alpha$ and $\beta\beta$ were identified (Fig. 5), although C_{32} hopanes were registered mainly in lignites. Samples S-By1 and S-By2 show much higher concentrations of C_{29} hopanes and C_{31} hopenes compared to the other studied material. The ratio of C_{30} $\beta\alpha$ moretane/$\alpha\beta$ hopane, used to determine thermal maturity of organic matter (Mackenzie et al., 1980; Seifert and Moldowan, 1986; Peters et al., 2005b), could be calculated for samples C-Or8, S-By2 and S-LW and is equal to 0.45, 0.18 and 0.27, respectively (Table 2). The ratio of the C_{31} $\beta\beta$ homohopane isomer to the sum of all isomers ($\beta\beta/(\beta\beta+\alpha\beta+\beta\alpha)$) is also an indicator of thermal maturity (Sinninghe Damstè et al., 1995; Farrimond et al., 1998). The values of $\beta\beta/(\beta\beta+\alpha\beta+\beta\alpha)$ in our study range from 0.15 to 0.55 (Table 2). Both the presence of $\beta\beta$ isomers and values of $\beta\alpha$ moretane/$\alpha\beta$ hopane and $\beta\beta/(\beta\beta+\alpha\beta+\beta\alpha)$ indicate low thermal maturity of the studied samples.

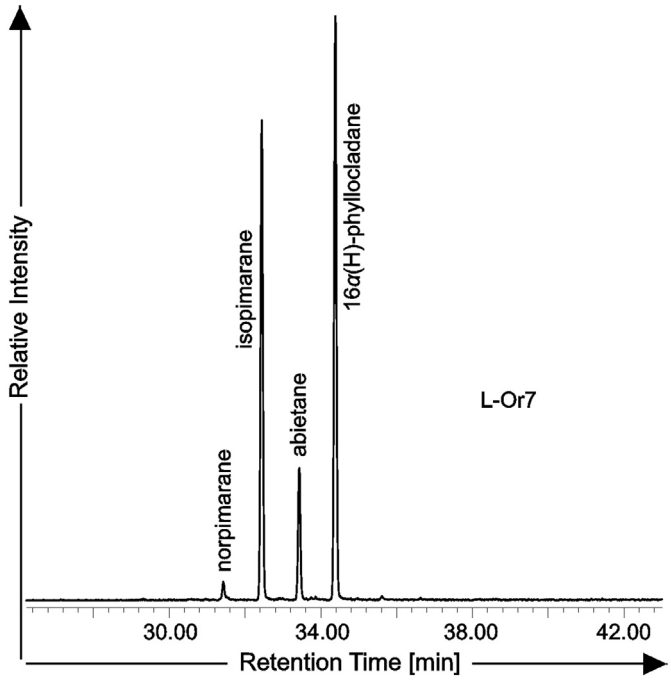

Fig. 4. Gas chromatogram (m/z = 123) showing the typical diterpenoid distribution for the investigated samples.

4.5. Steroids

C_{27}, C_{28}, C_{29} steranes and unsaturated steroids (sterenes and steradienes) were identified. The distribution of steroids demonstrates a C_{29} compounds predominance (Fig. 6). Among cholestanes and stigmastanes, both isomers, R and S, of the $\alpha\alpha\alpha$ configuration were present, whereas C_{28} sterane (ergostane) is represented by $\alpha\alpha\alpha$ (R) isomer, only. Cholestanes and ergostanes are more abundant in siltstones.

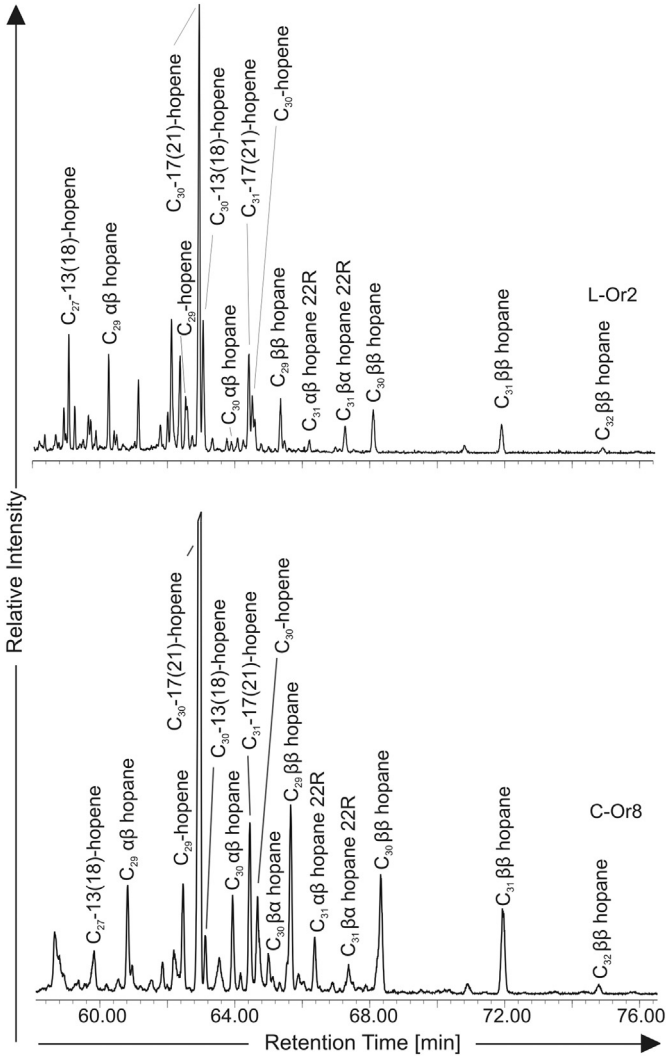

Fig. 5. Gas chromatograms (m/z = 191) of the pentacyclic hopanoid triterpenoids distribution of the samples L-Or2 and C-Or8.

The sterane 20S C_{29} *ααα* to the sum of isomers 20S and 20R [20S/(20S + 20R)] (e.g., Mackenzie and McKenzie, 1983; Beaumont et al., 1985; Seifert and Moldowan, 1986; Farrimond et al., 1998) ratio values range from 0.13 to 0.34, with the highest values calculated for the samples from Orava Lake (L-NU1 and L-NU2) and the lowest for the siltstones (Table 2). For the most samples the ratio of sterane to sterene for C_{27}, C_{28} and C_{29} compounds (Amo et al., 2007) ranges from 0.05 to 0.40 (Table 2). Samples S-By1 and S-By2 were the exceptions, having sterane/sterene ratios of 0.91 and 0.58, respectively. Both parameters are indicators of rather low organic matter thermal maturity.

The ratio of regular steranes vs. *αβ* hopanes allows the estimation of the origin of organic matter. Regular steranes are calculated as the sum of C_{27}, C_{28} and C_{29} steranes with the *ααα* and *αββ* configurations (both, R and S isomers are included), while *αβ* hopanes are determined by the sum of C_{29}-C_{33} hopanes (R + S isomers), having the *αβ* configuration (Tissot and Welte, 1984; Moldowan et al., 1985; Peters et al., 2005b). The ratio ranges from 0.28 to 0.96, except for sample L-Or10, which has a significantly lower value (0.004) (Table 2), which undoubtedly indicates terrestrial origin of examined organic matter.

4.6. Aromatic non-hopanoid terpenoids

Numerous derivatives of chrysene and picene, mostly representing the des-A degraded and aromatized or aromatized products of

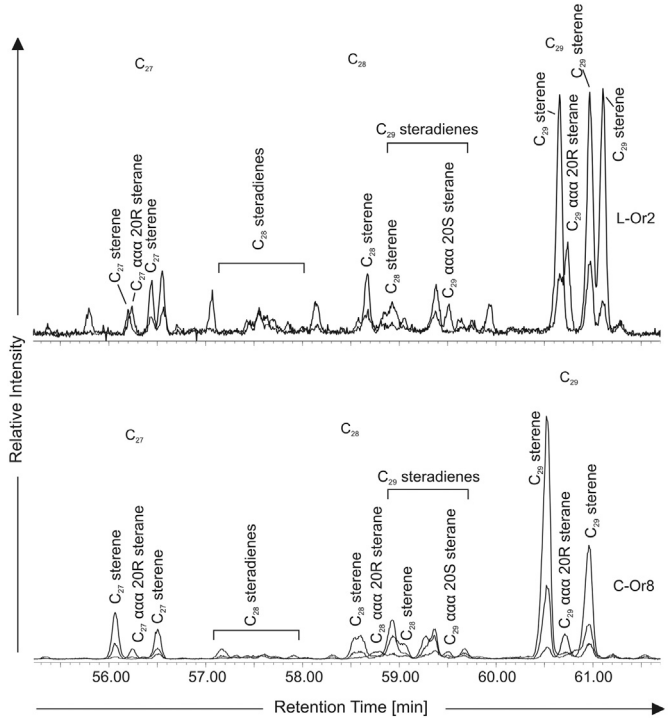

Fig. 6. Gas chromatograms (upper m/z = 215 + 217, lower m/z = 108 + 215 + 217) of the steroids distribution of the samples L-Or2 and C-Or8.

triterpenoids with oleanane and ursane skeleton were present in all the samples, except of sample C-CO. Trimethyltetrahydro- and tetramethyloctahydrochrysenes were identified, together with dimethyl- and trimethyltetrahydropicenes and tetramethyloctahydropicenes (Fig. 7). The most common compounds were 2,2,9-trimethyl-1,2,3,4-tetrahydropicene, 3,3,7-trimethyl-1,2,3,4-tetrahydrochrysene and isomers of 3,3,7,12a-tetramethyl-1,2,3,4,4a,11,12,12a-octahydrochrysene of an unknown exact structure. Chrysene and picene derivatives are more abundant in lignites than in clastic rocks. Other triterpenoid constituents of aromatic fraction are dinoroleana(ursa)-1,3,5(10),12-tetraene, dinoroleana(ursa)-1,3,5(10)-triene and aromatic triterpene with an open C-ring (Fig. 7). Amounts of total oleanane, ursane and lupane derivatives are quite uniform in lignites (usually around 40–50% of aromatic fraction) but highly variable in the clastics (constituting from few to over 70% of aromatic fraction).

The Average Aromatic Ring (AAR) value reflects the mean number of aromatic rings in the oleanane derivatives. It can provide information about the oxygen availability during sedimentation (Huang et al., 2013). The AAR calculated according to the formula defined by Huang et al. (2013) ranges from 3.89 to 4.00 in the samples examined (Table 3), leading to the conclusion that there was a high microbial activity in the sediment.

Aromatic derivatives of diterpenoids, such as retene, simonellite, dehydroabietane and abietatetraene were present in the samples studied, mainly in lignites. For some samples cadalene in relatively high concentrations has been determined.

The ratio of diterpenoids to the sum of diterpenoids and triterpenoids originating from angiosperms, can determine the relative gymno- and angiosperm contribution to the primary organic matter (Bechtel et al., 2007). The diterpenoids taken into consideration in this ratio are ent-beyerane, 16*α*(H)-phyllocladane, 16*β*(H)-phyllocladane, norabietane, pimarane, abietane, 19-norabieta-3,8,11,13-tetraene, 19-norabieta-8,11,13-triene, abieta-6,8,11,13-tetraene, simonellite and retene. Triterpenoids originating from angiosperms are understood as the sum of des-A-oleanenes, des-A-lupanes, olean-12-ene, olean-13(18)-

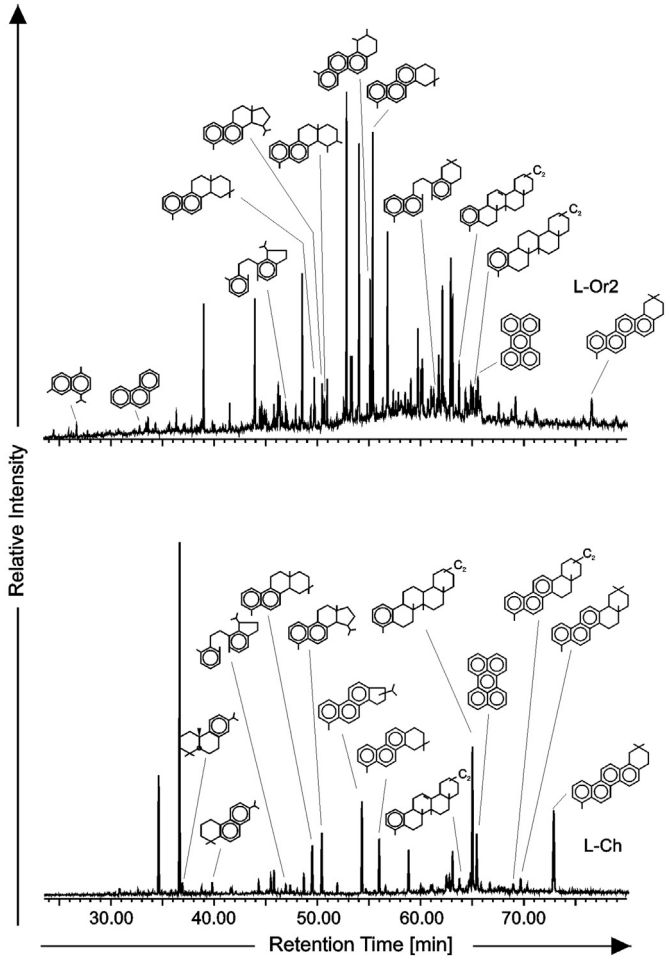

Fig. 7. Gas chromatograms (Total Ion Current) showing the aromatic fractions of the samples L-Or2 and L-Ch.

Table 3
Huminite reflectance and calculated aromatic biomarker parameters for the samples studied.

Sample	R_o [%]	AAR	CWDI	di- / (di- + triterpenoids)
L-Or7	–	3.98	0.98	0.04
L-Or1	0.20	3.95	0.93	0.01
L-Or2	0.26	3.94	0.85	0.01
L-Or10	–	3.96	0.27	0.21
L-Sy	–	3.91	0.73	0.12
L-Ch	–	4.00	0.88	0.10
L-CD	0.43	3.91	0.97	0.004
L-NU1	–	3.97	0.90	0.03
L-NU2	–	3.98	0.09	0.24
C-Or4	–	–	–	–
C-Or8	–	4.00	–	0.02
C-Ch	–	–	–	–
C-CO	–	–	–	–
C-CD	–	3.96	–	0.30
S-By1	–	4.00	–	0.05
S-By2	–	3.91	–	0.04
S-LW	–	3.89	–	0.10

R_o = Huminite reflectance.
AAR = Average Aromatic Ring (Huang et al., 2013).
CWDI = Conifer Wood Degradation Index (Marynowski et al., 2013).
di- / di- + triterpenoids = ratio of diterpenoids to the sum diterpenoids and angiosperm-derived triterpenoids (Bechtel et al., 2007).

ene, urs-12-ene, tetramethyloctahydrochrysenes, trimethyltetrahydrochrysenes, 24,25-dinoroleana-1,3,5(10),12-tetraene, 24,25-dinorursa-1,3,5(10),12-tetraene, 24,25,26-trisnorlupa-1,3,5(10)-triene, tetramethyloctahydropicenes, dimethyltetrahydropicenes and trimethyltetrahydropicenes (Bechtel et al., 2007). This ratio ranges from 0.004 to 0.30 in the samples examined (Table 3).

4.7. Perylene and other PAHs

Perylene is present in relatively high concentrations, especially in the clastic samples (Fig. 7). Other polycyclic aromatic hydrocarbons (PAHs) were also found, although in relatively small amounts: anthracene (mostly in lignites), pyrene and fluoranthene (mostly in clastic rocks), phenanthrene and its methyl derivatives (Fig. 7). Another phenanthrene derivative, 1-methylisopropyl-7,8-cyclopentenophenanthrene, is also present in the studied samples, with a significantly higher abundance in lignite samples.

For lignite samples, the Conifer Wood Degradation Index (CWDI) was calculated according to the following formula:

CWDI = perylene/(perylene + cadalene + retene + simonellite + dehydroabietane) (Marynowski et al., 2013).

The CWDI is an indicator of the degree of wood decay in sediments driven by wood-degrading fungi (Marynowski et al., 2013). The CWDI ranges from 0.73 to 0.98, except for the samples L-NU2 and L-Or10 where CWDI is 0.09 and 0.27, respectively (Table 3).

4.8. Polar compounds

In all samples including lignites, claystones and siltstones, long-chain *n*-fatty acids (> *n*-C_{23}) and long-chain *n*-alkanols predominates. In case of some lignites (L-Or1 and L-Or2), succinic acid as well as *n*-C_{16} and *n*-C_{18} *n*-fatty acids are important constituents of polar fraction as well. Significant group of polar compounds in majority of the samples are phenols, phenolic acids, ketones and aldehydes characteristic for both angiosperm and gymnosperm lignin degradation products. In that group vanillin, hydroxyacetophenone, syringaldehyde as well as benzoic, 3- and 4-hydroxybenzoic, vanillic, protocatechuic and syringic acid are major compounds (Fig. 8). Degradation products of cellulose and possibly also hemicellulose (e.g. Marynowski et al., 2018) are much less common, but *α*- and *β*-glucose, *α*- and *β*-arabinose and *α*- and *β*-arabinofuranose has been identified in two lignite samples (L-Or1 and L-Or2), and one siltstone (S-By1; Fig. 8). Polar diterpenoid biomolecules, including ferruginol and sugiol (e.g. Otto and Simoneit, 2001) are rare and were found in one lignite sample only (L-Ch). Dehydroabietic acid is more common, but its relative abundances except two samples (L-Or7 and L-Or10) are small. Polar triterpenoid natural products identified in lignite samples are quite common *α*- and *β*-amyrins. Sterols represented by *β*-sitosterol and stigmastanol are common polar components present in investigated rocks.

4.9. Huminite reflectance

Huminite reflectance (R_o) was measured in three lignite samples. L-Or1 and L-Or2 samples exhibit similar values of 0.20% (s.d. 0.06) and 0.26% (s.d. 0.04), respectively, while L-CD shows a slightly higher reflectance of 0.43% (s.d. 0.10) (Table 3). The distribution of measured R_o values was monomodal for each sample examined.

5. Discussion

5.1. Secondary processes

Weathering causes various modifications of organic matter on a molecular level. During weathering, TOC content decreases, and the vitrinite reflectance values and distributions of *n*-alkanes, steranes and hopanes are also altered (e.g., Faure et al., 1999; Elie et al., 2000; Marynowski et al., 2011a). One of the most important changes is an increase in short-chain *n*-alkanes and a decrease in long-chain *n*-alkane

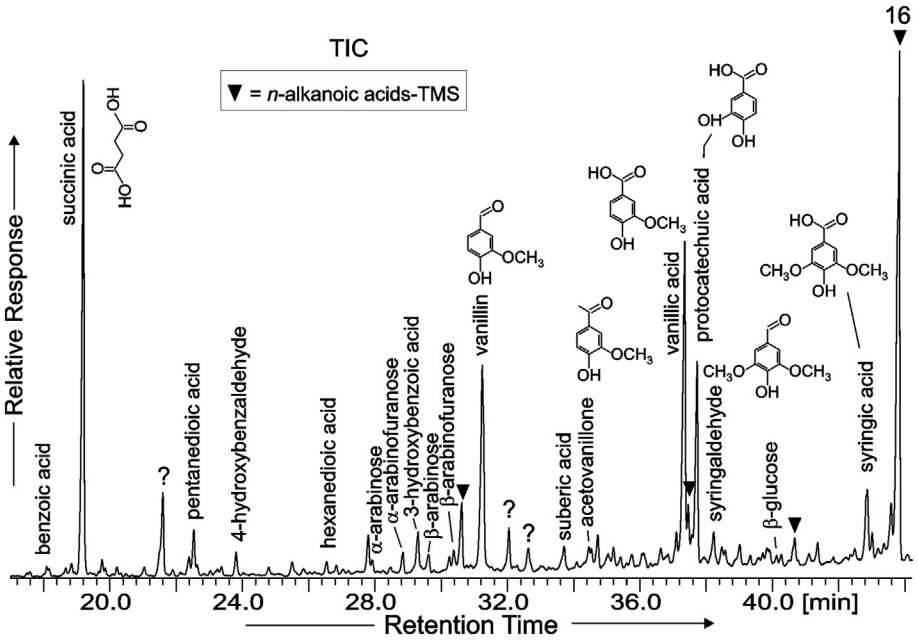

Fig. 8. Total Ion Current (TIC) of the silylated polar fraction (L-OR1 sample) showing the predominance of succinic acid and *n*-C_{16} alkanoic acid and the occurrence of benzoic acids typical for lignin decomposition.

concentrations. Moreover, aromatic terpenoids such as simonellite, cadalene or retene are eliminated. Weathering causes a decrease of perylene concentration and an increase of other PAHs such as phenanthrene and its methyl derivatives or fluoranthene (Marynowski et al., 2011b). Considering the predominance of long-chain and the scarcity of short-chain *n*-alkanes, the presence of aromatic terpenoids, perylene and small amounts of phenanthrenes and fluoranthene, no evidence of weathering was found in the samples examined. Nevertheless, the absence of weathering cannot be assumed with certainty, as it has been proven, that weathering can remove even over 25% of primarily present soluble organic matter, although highest values are obtained in dry, hot climates (Leythaeuser, 1973; Littke et al., 1991). Littke et al. (1991) have estimated that the organic carbon loss in Posidonia Shale in north Germany ammounted up to 16 wt%. Considering the general similarity of climate between northern Germany and southern Poland we could assume similar values. This could explain the relatively low TOC in lignites. Moreover, the prevalence of the polar fraction in the samples examined also indicates that they could have undergone some changes, as weathering depletes the organic matter in bitumen, especially aromatic hydrocarbons (Leythaeuser, 1973; Littke et al., 1991).

Biodegradation removes many compounds from organic matter, preferably *n*-alkanes, isoprenoids, C_{27}-C_{29} steranes and C_{30}-C_{35} hopanes. The reworking of organic matter by microorganisms results in the production of an unresolved complex mixture (UCM) visible on chromatograms (e.g., Gough and Rowland, 1990; Killops and Al-Juboori, 1990). An UCM was identified in samples C-Or4 and C-CO, which were interpreted as floodplain deposits. Additionally, neither diterpenoids, steranes nor hopanes were identified in these samples. Short-chain *n*-alkanes and aromatics were also partially removed. All these peculiarities evokes a high level of biodegradation for these samples.

Water washing effects are similar to those caused by biodegradation. Therefore, it might be difficult to distinguish between the effects of these processes. Water washing removes many aromatic and aliphatic compounds from the organic matter. The characteristic result of this process is the removal of short-chain *n*-alkanes according to their solubility in water. This removal leads to the characteristic "cut" shape of *n*-alkanes distribution (Palmer, 1993), observed in all the samples (Figs. 2 and 3) and distorts the Pr/Ph ratio, as both compounds are also easily removed. Water washing effects were observed in all the samples.

5.2. Origin of organic matter and sedimentary environment

A high percentage of polar fraction observed in the samples examined (Table 1) is typical for immature type III kerogen (Killops and Killops, 2005). This is confirmed by the presence of lignin and cellulose degradation products in polar fraction and products of wax lipids decomposition (long chain *n*-alkanols and fatty acids) (e.g. Otto and Simoneit, 2001; Stefanova et al., 2002; Otto et al., 2005) but also the distribution of *n*-alkanes with high odd-over-even predominance maximizing at *n*-C_{27}, *n*-C_{29} or *n*-C_{31} (Figs. 2 and 3) characteristic for terrestrial organic matter with a predominance of higher plants (e.g., Bray and Evans, 1961; Connan and Cassou, 1980; Rieley et al., 1991; Killops and Killops, 2005). Additionally, CPI values higher than 1 and a SCh/LCh significantly lower than 1 support this view (Table 2) (e.g., Bray and Evans, 1961; Scalan and Smith, 1970; Tissot and Welte, 1984; Bourbonniere and Meyers, 1996; Peters et al., 2005b). In samples C-Or4, S-By1 and S-By2, AI values were higher than 0.5 (Table 2), suggesting grasses as the main source of organic matter. In other samples, organic matter is derived mainly from trees, as the dominant compound is *n*-C_{27} or *n*-C_{29} (Schefuss et al., 2003; Zhang et al., 2006). Odd *n*-alkanes of the range *n*-C_{21} – *n*-C_{25} are considered to originate from mosses, mainly from *Sphagnum* (Bechtel et al., 2007). A high *n*-C_{23}/*n*-C_{31} ratio is determined for a lot of samples (Table 2) and might argue for peatlands or flooded forest (Pancost et al., 2002). A relatively high amount of *n*-C_{22} in samples C-CO and L-Sy can be related to a presence of specific algae species (Ekpo et al., 2005; Wang et al., 2010).

The distribution of steranes with a C_{29} predominance (Fig. 6) confirms the higher plant origin of organic matter (Moldowan et al., 1985; Peters et al., 2005b) supported by a sitosterol, a typical higher plant natural product, predominance (Otto and Simoneit, 2001). The ratio of regular steranes to *αβ* hopanes lower than 1 (Table 2) suggests a land plant origin or an organic matter highly reworked by bacteria (Peters et al., 2005b); however, considering the *n*-alkane distribution, the former interpretation can be considered as the dominant factor. The presence of tri- and tetracyclic diterpenoids, such as abietane, pimarane, isopimarane, fichtelitene, rimuene, phyllocladane, kaurane,

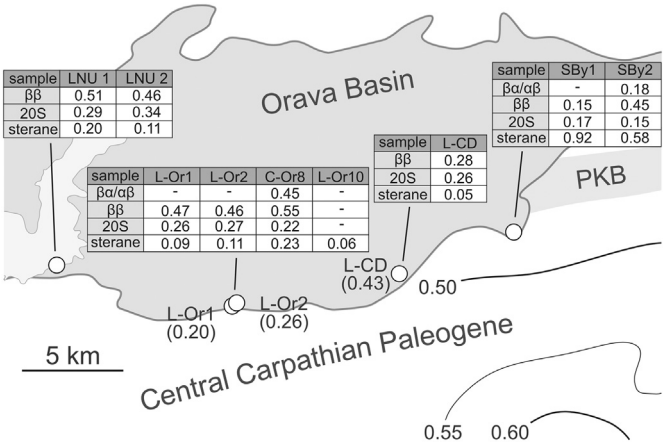

Fig. 9. Map of the estimated thermal maturity parameters for samples from the southern margin of the ONTB. Huminite reflectance values (%) are given in the brackets. Isolines of total random reflectivity (%) for the Podhale Synclinorium are estimated by Wagner (2011). Tables show biomarker-based maturity parameters:
βα/αβ = C_{30} moretane/hopane (Mackenzie et al., 1980), ββ = homohopane C31 ββ/(ββ + αβ + βα) (Sinninghe Damstè et al., 1995), 20S = C29 ααα sterane 20S/(20S + 20R) (Mackenzie and McKenzie, 1983), sterane = Σ(C27-C29 steranes)/Σ(C27-C29 sterenes) (Amo et al., 2007).

retene, simonellite and polar biomolecules like ferruginol, sugiol and dehydroabietic acid indicates gymnosperm plants as they originate from compounds present in gymnosperm resins (Wakeham et al., 1979; Dehmer, 1995; Hautevelle et al., 2005; Marynowski et al., 2013). Oleanane, ursane and lupane derivatives originate from the *β*-amyrin, *α*-amyrin and lupeol present in the leaves, bark and roots of angiosperms (Mille et al., 2006; Bechtel et al., 2007). Angiosperm origin of the studied organic matter could also be concluded from the presence of chrysene and picene derivatives, although their origin from *α*- and *β*-amyrin is not confirmed (Tuo and Philp, 2005). Inasmuch as both *β*-amyrin and *α*-amyrin were determined in lignite samples, chrysene and picene derivatives origin from these natural products is of great certitude. In order to recognize the relative input of gymno- and angiosperms to the primary organic matter, the di−/(di- + triterpenoids) ratio was calculated. For all the samples examined, the ratio is low (Table 3), which suggests that angiosperm plants were predominant (Bechtel et al., 2007), although the results should be considered with caution as it has been proved that, when compared to the proportions of their macroscopic remnants, gymnosperm-derived compounds are less abundant in a sediment than angiosperm biomarkers (Otto et al., 2005). Also the composition of polar fraction demonstrates relatively high abundances of gymnosperm organic matter. Considering these data, we find determining the prevalence of any of these plant groups impossible to state definitely.

The presence of hop-17(21)-enes (Fig. 5) is also important in terms of determining the organic matter source. Although their precursors are also present in bacteria and fungi, interpreting them as compounds derived from mosses and ferns seems reasonable, especially considering their high concentrations compared to other bacteria-derived hopanoids (Bechtel et al., 2007).

The Pr/Ph ratio in all samples is lower than 1 (Table 2), which indicates anoxic conditions during sedimentation (Didyk et al., 1978). These results should be taken with caution, as both pristane and phytane are prone to secondary alterations, and the Pr/Ph ratio in the lignites may not reflect the real redox conditions during the sedimentation (Connan, 1974; Kohnen, 1991; de Graaf et al., 1992; Peters et al., 2005b). Water washing surely has led to the partial removal of both pristane and phytane from the investigated samples, thus disturbing their original proportions. Redox conditions can also be determined using AAR, which rises with increasing oxidation potential in sediments (Huang et al., 2013). For the studied material, the AAR mean value is 3.95 (Table 3) which, compared to the published data, is relatively high and indicates high activity of aerobic bacteria and well oxidized sediment (Huang et al., 2013). Considering that water washing is present in all the samples and the influencing Pr/Ph, the AAR seems to be a more reliable indicator of redox conditions. High microbial activity is also indicated by the presence of the derivatives of chrysene and picene (Wakeham et al., 1979). In addition to bacteria, wood-degrading fungi were active during the early stage of diagenesis, as suggested by the presence of perylene and by the CWDI values > 0.7 (Table 3), which are characteristic for highly decomposed wood (Marynowski et al., 2013). It is rather surprising because in the case of the Miocene lignites, CWDI values are very small (Marynowski et al., 2013).

The presence of hop-13(18)-enes (Fig. 5) can also provide insight into the depositional conditions. They are most likely derived from alterations of hop-17(21)-enes in an acidic environment (Meredith et al., 2008; Pan et al., 2010). This interpretation appears to be appropriate, considering the high *n*-C_{23} amounts present in samples, indicating *Sphagnum* as one of the main constituents of plant communities in the studied area during the Neogene.

Pyrene, anthracene and fluoranthene occurring in many samples could have been formed by the incomplete burning of biomass and caustobiolites, e.g., during wildfires. These compounds can be transported by air- or waterborne processes and deposited in different locations (Killops and Massoud, 1992; Jiang et al., 1998; Marynowski and Simoneit, 2009). As these compounds are present in almost all the samples, although in small concentrations, it can be assumed that they were transported by riverine or eolian transport from different source areas rather than formed in situ.

5.3. Thermal maturity of organic matter

The huminite reflectance values (Table 3; Fig. 9) indicate an immature character of the organic matter, although the sample from the SE part of the basin (L-CD) shows a slightly higher maturity of the late diagenesis phase (R_o = 0.43%) (Peters and Moldowan, 2017). Thermal maturity can also be determined by biomarker-based indicators, such as CPI, which decreases to 1 with increasing maturity (e.g., Bray and Evans, 1961; Scalan and Smith, 1970). The CPI varies from 1.53 to 8.41 (Table 2), indicating that the organic matter examined is immature, with the minimum values representing the phase of early catagenesis. Direct correlation between CPI and R_o values in samples L-Or1, L-Or2 and L-CD is poor, which is probably related to the susceptibility of CPI to alterations caused by water washing and its dependence on the organic matter source (e.g., Palmer, 1993). Thus, maturity determined based on the CPI is probably overestimated.

The presence of unstable *ββ* hopane isomers (Fig. 5) indicates very low maturation of organic matter, generally below or around R_o = 0.4% (Nytoft and Bojesen-Koefoed, 2001; Peters and Moldowan, 2017). The C_{30} moretane/hopane (*βα/αβ*) ratio decreases from 0.8 to 0.15 with an increase in thermal maturation (e.g., Peters et al., 2005b). The ratio was possible to calculate for three samples (Table 2; Fig. 9) and their values (0.18, 0.27 and 0.45) indicate that two of them (C-Or8 and S-LW) are immature and one (S-By2) is mature (Nytoft and Bojesen-Koefoed, 2001). The *ββ/(ββ + αβ + βα)* homohopane C_{31} ratio decreases to 0 during increasing thermal maturation before the organic matter reaches the mature phase (Farrimond et al., 1998; Peters and Moldowan, 2017). This ratio ranges from 0.34 to 0.55 in most samples (Table 2; Fig. 9), indicating immature organic matter. The lowest values obtained in samples L-CD and S-By1 were 0.28 and 0.15, respectively. Other maturity indicators show concordantly that these samples were relatively deeply buried, so their elevated maturity seems reliable, especially for sample L-CD, which exhibits the highest R_o value. However, even samples L-CD and S-By1 should be treated as immature, with R_o not exceeding ca. 0.45% (see Peters and Moldowan, 2017).

The 20S/(20S + 20R) parameter based on the C_{29} *ααα* steranes is one of the most commonly used biomarker indicators of thermal maturity. Its values increase from 0 to 0.45–0.55 in clastic rocks and to 0.30–0.45 in lignites at the transition from diagenesis to catagenesis during increasing thermal maturation (Farrimond et al., 1998; Peters and Moldowan, 2017). In the clastic samples, the 20S/(20S + 20R) ranges from 0.13 to 0.26 (Table 2; Fig. 9), which means that they are immature. Lignites have slightly higher values, from 0.26 to 0.34 (Table 2; Fig. 9), which indicates a maturation stage of diagenesis and early catagenesis (Farrimond et al., 1998; Peters and Moldowan, 2017). The values of 20S/(20S + 20R) can be distorted by the presence of C_{29} sterenes and steradienes (Fig. 6) that were not yet transformed into steranes (Amo et al., 2007). The presence of those unsaturated steroids confirms the immature character of the organic matter. The steranes to sterenes ratio increases rapidly with increasing thermal maturity, from 0.2 to 0.9 at the temperature range between 45 and 55 °C (Amo et al., 2007). The ratio ranges from 0.05 to 0.92 (Table 2) in the samples examined, which implies that the samples have not reached the catagenesis (oil window) phase.

The stratigraphy in the ONTB is problematic and still poorly constrained, so it is difficult to assess the exact age relations between Nove Ústie, the Oravica River, the Czarny Dunajec River and the Bystry Stream sections. However, since they are located along the southern margin of the basin of the inferred highest magnitude of uplift (Łoziński et al., 2017), they presumably represent the basal part of the infill. Therefore, samples from these sections can be treated as roughly representing the same interval of the basin infill, and their thermal maturity parameters can be compared to reconstruct the history of subsidence, burial and exhumation along the *E*-W transect through the basin. Huminite reflectance values obtained from samples L-CD, L-Or1 and L-Or2 suggest a decrease in the maturation of sediments towards the west (Table 3; Fig. 9). This trend is confirmed by certain biomarker-based parameters. The *βα/αβ* ratio increases from 0.18 to 0.45 towards the west (Table 2; Fig. 9), similar to the case of the *ββ/(ββ + αβ + βα)* C_{31} homohopane ratio, which also tends to be lower in the eastern than in the western part of the basin. The only exception is sample S-By2, with a value of *ββ/(ββ + αβ + βα)*, similar to the western samples (Table 2; Fig. 9), most likely due to a higher influence of secondary processes such as water washing or biodegradation. The sterane/sterene ratio also generally decreases to the west (Table 2; Fig. 9), although this trend is not that clear due to large spread of values, even in a single section, e.g., between S-By1 (0.92) and S-By2 (0.58). All these biomarker-based indices clearly indicate a lower thermal maturity in the western part of the basin. The only biomarker-based parameter not following the described trend is 20S/(20S + 20R), which shows an increase in values in the direction opposite from what was suspected, i.e., from east to west (Table 2; Fig. 9). As mentioned above, it is difficult to expect reliable results based on the 20S/(20S + 20R) ratio with such a high contribution of sterenes, in the overall steroid composition of the samples examined.

Waliczek and Solecki (2014) measured the vitrinite reflectance in a claystone from Chochołów, which is the same area as the section of the Czarny Dunajec Stream examined in this work. They obtained a R_o value of 0.37%, which is very similar to our result (0.43%) from that locality and confirms the increased maturity of sediments in the SE part of the ONTB. However, Nagy et al. (1996) obtained relatively high R_o values for lignites from the SW part of the basin in Nove Ústie (from 0.35% to 0.43%), which contrasts with our biomarker-based results obtained for lignites from the same locality and does not fit the westward trend of maturity decrease. Such a discrepancy can relate to a partial oxidation of lignites from the Nove Ústie site, which influenced the vitrinite reflectance measurement. As it was shown, organic matter weathering can increase R_o values up to 0.2% (Marynowski et al., 2011b). If so, the R_o values obtained by Nagy et al. (1996) are not representative of burial conditions, and the extremely high calculated geothermal gradient of 50 °C/km is overestimated.

5.4. Magnitude and timing of exhumation

The Magura Nappe sediments near the northern margin of the ONTB were estimated to be heated up to 105 °C, but it is estimated that most of the sediments (4,4 km) had been eroded before the onset of Neogene sedimentation (Świerczewska, 2005), so the Magura Nappe in the region represents a different stage of thermal history. Thermal maturity of the PS, on the other hand, decreases from SE to NW, which is manifested by the decreasing illite/smectite ratio (Środoń et al., 2006) and vitrinite reflectance (Wagner, 2011) measured for Paleogene sedimentary rocks (Fig. 9). The lowest R_o values of ~0.5% occur close to the junction between the PS, PKB and ONTB near Chochołów (Fig. 9). They are significantly lower than those reported for the Aalenian and Bajocian samples from the Szlachtowa and the Czorsztyn formations from the PKB (~1.0%) (Wagner, 2011) and for the High- and Sub-Tatric units (Ladynian to Tythonian in age) to the south of the PS (0.9–1.8%; Poprawa et al., 2002). However, the R_o value obtained in this study for the sample from Czarny Dunajec (L-CD) in the SE part of the ONTB (0.43%) is only slightly lower than that obtained by Wagner (2011) for a Paleogene sample from the nearby Chochołów (0.49%) in the NE part of the PS (Fig. 9). Marynowski et al. (2006) obtained values of ~ 0.6% of the calculated vitrinite reflectance for the samples from the Chochołów PIG-1 well from the depth of 280 to 600 m. Moreover, the thermal maturity of the samples collected along the southern margin of the ONTB decreases to the west, similar to the trend in the PS, where the thermal maturity decreases to the NW (Środoń et al., 2006; Wagner, 2011). This shows that the trend of decreasing thermal maturity in the PS continues without a gap in the ONTB (Fig. 9). This suggests that the burial histories of the ONTB and Podhale Basin could have been associated and that rocks in both basins could have experienced maximum burial during the same period. However, this scenario is not supported by the thermochronological investigations, which indicate that the maximum burial in the NW part of the Podhale Basin occurred between 15.8 and 17.1 Ma (Środoń et al., 2006). This is earlier than the onset of deposition in the ONTB that has recently been dated with U—Pb dating of zircons from a tuffite at ~12 Ma (Wysocka et al., 2018). Thus, maximum burial and the subsequent partial erosion of the Podhale Basin must have occurred prior to sedimentation in the ONTB. Then, after the period of subsidence and deposition, the ONTB experienced uplift and exhumation during the Pliocene/Quaternary, which continues (Vanko, 1988). Thus, the apparent continuity of thermal maturity between the PS and ONTB must be coincidental.

Still, the fact that the trend of increasing maturity and the amount of erosion to the SE continues through both units (Fig. 9) is intriguing and leads to some conclusions about the exhumation history of both units. After the initial Middle Miocene phase of exhumation, probably related to the Savic phase of the Alpine orogeny, the western part of the Podhale Basin experienced subsidence and was covered by Upper Miocene-Pliocene sediments belonging to the ONTB. Thickness of these deposits near Chochołów could have been close to the amount of the exhumation of the Podhale Basin, as there is no significant difference between thermal maturity of the neighboring PS and ONTB. The exhumation magnitude of PS is highest near the Ružbachy Fault, which suggests that this fault played an important tectonic role during the uplift of the PS in the Miocene (Środoń et al., 2006). Interestingly, this trend continues in the ONTB, which may be attributed in this area to the Pliocene/Quaternary dip-slip activity of the strike-slip Krowiarki Fault (also: Orava Fault, e.g., Baumgart-Kotarba et al., 2004, Łoziński et al., 2017).

The thermal maturity of surface samples, and hence the amplitude of the uplift and exhumation, decrease to the NW in both basins (Fig. 9). The highest R_o value (0.43%) obtained in this study for the SE margin of the ONTB suggests that the temperature of maturation (if the peak temperature was reached due to maximal burial) was probably in the range of 45–65 °C, depending on the model applied (Barker and Pawlewicz, 1994; Hunt, 1995). This sample was collected from an outcrop, so the difference between the maximum temperature of

maturation and the current mean temperature in the region does not exceed 35–55 °C. The amount of erosion associated with such a temperature drop can be estimated by assuming the thermal paleogradient for the Late Miocene. Środoń et al. (2006) indicated that the paleogradient in the Middle Miocene was 20–25 °C/km, which is similar to the present-day value of 19–23 °C/km (Środoń et al., 2006), while Nagy et al. (1996) suggested a much higher value of up to 50 °C/km for the Late Miocene. We cannot apply the paleogradient proposed by Środoń et al. (2006) because it is close to the present-day value, while the gradient must have been somewhat greater during the Late Miocene, as there was active volcanism present in the area, especially within PKB and Magura Nappe, related to reactivation of fault zones formed earlier (Nejbert et al., 2012; Anczkiewicz and Anczkiewicz, 2016). Although there is no evidence of magmatic activity in the ONTB, except one tuffite layer (Łoziński et al., 2015; Wysocka et al., 2018), the presence of andesites in the tectonic units surrounding and underlying the ONTB suggests an overall elevated gradient in the region. The paleogradient estimated by Nagy et al. (1996) is extremely high and may be overestimated, as discussed above. Moreover, it is difficult to assess the reliability of modeling that was used in the calculation. Thus, an intermediate value of 35 °C/km suggested by Wagner (2011) will be used in this work. The calculated maximum thickness of eroded strata is 1–1.6 km for the SE part of the Orava Basin, and this value decreases towards the west. Such a magnitude of exhumation at the present-day margin of the ONTB implies that the paleogeographic extent of the basin must have been much greater. Evidently, the area adjacent to the south that is currently composed of eroded rocks of the PS must have been covered with < 1.6 km thick Neogene deposits of the ONTB, which is similar to the estimations of Wagner (2011) of < 1 km.

6. Conclusions

Based on the molecular composition of organic matter and the geochemical indicators of the Neogene sediments in the Orava-Nowy Targ Basin, only type III kerogen was identified, which confirms that the sedimentation occurred in a continental setting. Higher plants, mainly grasses and trees, are indicated as the main source of organic matter. Considering the high input of peat–derived organic matter in most samples, such as *Sphagnum*-derived compounds, mixed swamp forests are proposed as the dominant plant community in the examined area, although other communities such as mixed forests and meadows, swamps and mires with a few trees were also present. The sedimentary environment of wetlands and floodplains was oxic and acidic, in which intensive activity of bacteria and fungi led to the partial decay of organic matter. Wildfires occurred in the examined area during the Neogene, as compounds such as pyrene, fluoranthene and anthracene were identified in most of the studied samples. The influence of water washing that disrupted the distribution of short-chain *n*-alkanes and acyclic isoprenoids is detectable in all the samples. Only two of the samples underwent biodegradation, which led to the removal of almost all the compounds from the aliphatic fraction and most compounds from the aromatic fraction. Signs of post-exhumation weathering were not identified.

The huminite reflectance of the examined samples ranges from 0.20 to 0.43%, proving the organic matter immaturity. The presence of unsaturated compounds and the values of calculated geochemical indicators also confirm it and denote that examined organic matter has not reached further than late diagenesis stage. A comparison of R_o and CPI indicates that the latter is a less reliable proxy of maturity due to water washing and its dependence on an organic matter source. The thermal maturity of samples collected from the basal part of sedimentary infill along the southern margin of the ONTB exhibits a clear decreasing trend towards the west. Moreover, the comparison of different biomarker-based thermal maturity indicators from samples located at the southern margin of the basin allowed estimation of the applicability of different thermal maturity indices to relatively immature terrigenous sediments. The C_{30} $\beta\alpha/\alpha\beta$ hopane, $\beta\beta/(\beta\beta + \alpha\beta + \beta\alpha)$ homohopane and sterane/sterene ratios show good correlations with the maturity trend based on the huminite reflectance.

The deepest buried samples were heated to a maximum temperature of ~45–65 °C, temperatures of late diagenesis-early catagenesis. Therefore, erosion must have removed 1–1.6 km of sediments in the SE part of the basin, where the outcrops of these strata and their contact with the basement is observed. Thermal maturity of samples representing the basal interval of the ONTB infill that are currently on the surface decreases to the west, which indicates that the amount of exhumation decreased in this direction. These results clearly imply that the ONTB extended beyond its current limits, at least in the southern part, and must have covered the rocks of the PS that are currently exposed. The Neogene sediments belonging to the ONTB must have formed the 1–1.6 km thick cover on the western part of PS.

Acknowledgements

This work was supported by the National Science Centre (NCN) [grants number 2011/01/B/ST10/07591 and 2015/19/B/ST10/00925] and Institute of Geological Sciences, Polish Academy of Sciences. We would like to thank two anonymous reviewers whose constructive comments and insightful suggestions greatly improved the manuscript.

References

Amo, M., Suzuki, N., Shinoda, T., Ratnayake, N.P., Takahashi, K., 2007. Diagenesis and distribution of sterenes in Late Miocene to Pliocene marine siliceous rocks from Horonobe (Hokkaido, Japan). Org. Geochem. 38, 1132–1145.
Anczkiewicz, A.A., Anczkiewicz, R., 2016. U–Pb zircon geochronology and anomalous Sr–Nd–Hf isotope systematics of late orogenic andesites: Pieniny Klippen Belt, Western Carpathians, South Poland. Chem. Geol. 427, 1–16.
Barker, C.E., Pawlewicz, M.J., 1994. Calculation of vitrinite reflectance from thermal histories and peak temperature: a comparison of methods. In: Chapter 14, Vitrinite Reflectance as a Maturity Parameter. American Chemical Society, pp. 216–229.
Bastow, T.P., Van Aarssen, B.G.K., Lang, D., 2007. Rapid small-scale separation of saturate, aromatic and polar components in petroleum. Org. Geochem. 38, 1235–1250.
Baumgart-Kotarba, M., 1996. On origin and age of the Orava Basin, West Carpathians. Studia Geomorphologica Carpatho-Balcanica 30, 101–116.
Baumgart-Kotarba, M., 2001. Continuous tectonic evolution of the Orava basin from Late Badenian to the present-day. Geol. Carpath. 52, 103–110.
Baumgart-Kotarba, M., Marcak, H., Marton, E., Imre, G., 2004. Rotation along transverse transforming Orava strike-slip fault in the light of geomorphological, geophysical and paleomagnetic data (Western Carpathians). Geol. Carpath. 55, 219–226.
Beaumont, C., Boutlier, R., Mackenzie, A.S., Rullkötter, J., 1985. Isomerization and aromatization of hydrocarbons and the paleothermometry and burial history of Alberta Foreland Basin. Am. Assoc. Pet. Geol. Bull. 69, 546–566.
Bechtel, A., Reischenbacher, D., Sachsenhofer, R.F., Gratzer, R., Lücke, A., 2007. Paleogeography and paleoecology of the upper Miocene Zillingdorf lignite deposit (Austria). Int. J. Coal Geol. 69, 119–143.
Birkenmajer, K., 1960. Geology of the Pieniny Klippen Belt of Poland. Jahrb. Geol. Bundesanst. 103, 1–36.
Birkenmajer, K., Oszczypko, N., 1989. Cretaceous and Palaeogene lithostratigraphic units of the Magura Nappe, Krynica Subunit, Carpathians. Ann. Soc. Geol. Pol. 59, 145–181.
Bourbonniere, R.A., Meyers, P.A., 1996. Sedimentary geolipid records of historical changes in the watersheds and productivities of Lakes Ontario and Erie. Limnol. Oceanogr. 41, 352–359.
Bray, E.E., Evans, E.D., 1961. Distribution of n-paraffins as a clue to recognition of source beds. Geochim. Cosmochim. Acta 22, 2–15.
Cieszkowski, M., Oszczypko, N., Zuchiewicz, W., 1989. Upper Cretaceous siliciclastic carbonate turbidites at Szczawa, Magura Nappe, West Carpathians, Poland. Bulletin of the Polish Academy of Sciences, Earth Sciences 37, 231–245.
Connan, J., 1974. Time-temperature relation in oil genesis. Am. Assoc. Pet. Geol. Bull. 58, 2516–2521.
Connan, J., Cassou, A.M., 1980. Properties of gases and petroleum liquids derived from terrestrial kerogen at various maturation levels. Geochim. Cosmochim. Acta 44, 1–23.
de Graaf, W., Sinninghe Damstè, J.S., de Leeuw, J.W., 1992. Laboratory simulation of natural sulphurization: I. Formation of monomeric and oligomeric isoprenoid polysulphides by low-temperature reactions of inorganic hydrogen polysulphides with phytol and phytadienes. Geochim. Cosmochim. Acta 56, 4321–4328.
Dehmer, J., 1995. Petrological and organic geochemistry investigation of recent peats with known environment of deposition. Int. J. Coal Geol. 28, 111–138.
Didyk, B.M., Simoneit, B.R.T., Brassell, S.C., Eglinton, G., 1978. Organic geochemical indicators of palaeoenvironmental conditions of sedimentation. Nature 272,

216–222.
Ekpo, B.O., Oyo-Ita, O.E., Wehner, H., 2005. Even-*n*-alkane/alkene predominances in surface sediments from the Calabar River, SE Niger Delta, Nigeria. Naturwissenschaften 92, 341–346.
Elie, M., Faure, P., Michels, R., Landais, P., Griffault, L., 2000. Natural and laboratory oxidation of low-organic-carbon-content sediments: comparison of chemical changes in hydrocarbons. Energy Fuel 14, 854–861.
Farrimond, P., Taylor, A., Telnæs, N., 1998. Biomarker maturity parameters: the role of generation and thermal degradation. Org. Geochem. 29, 1181–1197.
Faure, P., Landais, P., Griffault, L., 1999. Behavior of organic matter from Callovian shales during low-temperature air oxidation. Fuel 78, 1515–1525.
Garecka, M., 2005. Calcareous nannoplankton from the Podhale Flysch (Oligocene-Miocene, Inner Carpathians, Poland). Studia Geologica Polonica 124, 353–370.
Goossens, H., de Leeuw, J.W., Schenck, P.A., Brassell, S.C., 1984. Tocopherols as likely precursors of pristine in ancient sediments and crude oils. Nature 312, 440–442.
Gough, M.A., Rowland, S.J., 1990. Characterisation of unresolved complex mixtures of hydrocarbons in petroleum. Nature 344, 648–650.
Hautevelle, Y., Michels, R., Malarte, F., Trouiller, A., 2005. Vascular plant biomarkers as ancient vegetation proxies and their stratigraphic use for tracing palaeoclimatic changes during Jurassic in Western Europe. Geophysical Research Abstracts 7.
Huang, X., Xue, J., Wang, X., Meters, P.A., Huang, J., Xie, S., 2013. Paleoclimate influence on early diagenesis of plant triterpenes in the Dajiuhu peatland, Central China. Geochim. Cosmochim. Acta 123, 106–119.
Hunt, J.M., 1995. Petroleum Geochemistry and Geology, 2 ed. W.H. Freeman and Co., New York.
Jiang, C., Alexander, R., Kagi, R.I., Murray, A.P., 1998. Polycyclic aromatic hydrocarbons in ancient sediments and their relationships to palaeoclimate. Org. Geochem. 29, 1721–1735.
Killops, S.D., Al-Juboori, M.A.H.A., 1990. Characterisation of the unresolved complex mixture (UCM) in the gas chromatograms of biodegraded petroleums. Org. Geochem. 15, 147–160.
Killops, S., Killops, V.J., 2005. An Introduction to Organic Geochemistry, 2nd edition. Blackwell Publishing, Malden.
Killops, S.D., Massoud, M.S., 1992. Polycyclic aromatic hydrocarbons of pyrolitic origin in ancient sediments: evidence for vegetation fires. Org. Geochem. 18, 1–7.
Kohnen, M.E.L., 1991. Sulphurised lipids in sediments: the key to reconstruct paleobiochemicals and their origin. Ph. D. Thesis. Universiteit Delft, Delft, the Netherlands.
Kováč, P., Hók, J., 1993. The Central Slovak Fault System – the field evidence of a strike slip. Geol. Carpath. 44, 155–159.
Kováč, M., Nagymarosy, A., Oszczypko, N., Csontos, L., Ślączka, A., Marunteanu, M., Matenco, L., Márton, E., 1998. Palinspastic reconstruction of the Pannonian–Carpathian region during the Miocene. In: Rakús, M. (Ed.), Geodynamic Development of the Western Carpathians. Geological Survey of Slovak Republic, Bratislava, pp. 189–217.
Leythaeuser, D., 1973. Effects of weathering on organic matter in shales. Geochim. Cosmochim. Acta 37, 113–120.
Littke, R., Klussmann, U., Krooss, B., Leythaeuser, D., 1991. Quantification of loss of calcite, pyrite, and organic matter due to weathering of Toarcian black shales and effects on kerogen and bitumen characteristics. Geochim. Cosmochim. Acta 55, 3369–3378.
Łoziński, M., Wysocka, A., Ludwiniak, M., 2015. Neogene terrestrial sedimentary environment of the Orava-Nowy Targ Basin: a case study of the Oravica River section near Čimchová, Slovakia. Geological Quarterly 59, 21–34.
Łoziński, M., Ziółkowski, P., Wysocka, A., 2017. Tectono-sedimentary analysis using the anisotropy of magnetic susceptibility: the study of terrestrial and freshwater Neogene of the Orava Basin. Geol. Carpath. 68, 479–500.
Mackenzie, A.S., McKenzie, D., 1983. Isomerization and aromatization of hydrocarbons in sedimentary basins formed by extension. Geol. Mag. 120, 417–470.
Mackenzie, A.S., Patience, R.L., Maxwell, J.R., Vandenbroucke, M., Durand, B., 1980. Molecular parameters of maturation in the Toarcian shales, Paris Basin, FranceI. Changes in the configurations of acyclic isoprenoid alkanes, steranes, and triterpanes. Geochim. Cosmochim. Acta 44, 1709–1721.
Marynowski, L., Simoneit, B.R.T., 2009. Widespread Late Triassic to Early Jurassic wildfire records from Poland: evidence from charcoal and pyrolytic polycyclic aromatic hydrocarbons. PALAIOS 24, 785–798.
Marynowski, L., Gawęda, A., Poprawa, P., Żywiecki, M.M., Kępińska, B., Merta, H., 2006. Origin of organic matter from tectonic zones in the Western Tatra Mountains Crystalline Basement, Poland: an example of bitumen – source rock correlation. Mar. Pet. Geol. 23, 261–279.
Marynowski, L., Kurkiewicz, S., Rakociński, M., Simoneit, B.R.T., 2011a. Effects of weathering on organic matter: I. Changes in molecular composition of extractable organic compounds caused by paleoweathering of a Lower Carboniferous (Tournaisian) marine black shale. Chem. Geol. 285, 144–156.
Marynowski, L., Szełęg, E., Jędrysek, M.O., Simoneit, B.R.T., 2011b. Effects of weathering on organic matter: II. Fossil wood weathering and implications for organic geochemical and petrographic studies. Org. Geochem. 42, 1076–1088.
Marynowski, L., Smolarek, J., Bechtel, A., Phillipe, M., Kurkiewicz, S., Simoneit, B.R.T., 2013. Perylene as an indicator of conifer fossil wood degradation by wood-degrading fungi. Org. Geochem. 59, 143–151.
Marynowski, L., Bucha, M., Smolarek, J., Wendorff, M., Simoneit, B.R.T., 2018. Occurrence and significance of mono-, di- and anhydrosaccharide biomolecules in Mesozoic and Cenozoic lignites and fossil wood. Org. Geochem. 116, 13–22.
Meredith, W., Snape, C.E., Carr, A.D., Nytoft, H.P., Love, G.D., 2008. The occurrence of unusual hopenes in hydropyrolysates generated from severely biodegraded oil seep asphaltenes. Org. Geochem. 39, 1243–1248.
Mille, G., Guiliano, M., Asia, L., Malleret, L., Jalaluddin, N., 2006. Sources of hydrocarbons in sediments of the Bay of Fort de France (Martinique). Chemosphere 64, 1062–1073.
Milner, C.W.D., Rogers, M.A., Evans, C.R., 1977. Petroleum transformations in reservoirs. J. Geochem. Explor. 7, 101–153.
Moldowan, J.M., Seifert, W.K., Gallegos, E.J., 1985. Relationship between petroleum composition and depositional environment of petroleum source rocks. Am. Assoc. Pet. Geol. Bull. 69, 1255–1268.
Nagy, A., Vass, D., Petrik, F., Pereszlényi, M., 1996. Tectogenesis of the Orava Depression in the light of latest biostratigraphic investigations and organic matter alteration studies. Slovak Geological Magazine 1, 49–58.
Nejbert, K., Jurewicz, E., Macdonald, R., 2012. Potassium-rich magmatism in the Western Outer Carpathians: Magmagenesis in the transitional zone between the European Plate and Carpathian–Pannonian region. Lithos 146-147, 34–47.
Nytoft, H.P., Bojesen-Koefoed, J.A., 2001. 17α, 21α(H)-hopanes: natural and synthetic. Org. Geochem. 32, 841–856.
Oszast, J., Stuchlik, L., 1977. The Neogene vegetation of the Podhale (West Carpathians, Poland) (in Polish with English summary). Acta Palaeobotanica 18, 45–86.
Otto, A., Simoneit, B.R.T., 2001. Chemosystematics and diagenesis of terpenoids in fossil conifer species and sediment from the Eocene Zeitz formation, Saxony, Germany. Geochim. Cosmochim. Acta 65, 3505–3527.
Otto, A., Simoneit, B.R.T., Rember, W.C., 2005. Conifer and angiosperm biomarkers in clay sediments and fossil plants from the Miocene Clarkia formation, Idaho, USA. Org. Geochem. 36, 907–922.
Palmer, S., 1993. Effect of biodegradation and water washing on crude oil composition. In: Engel, M.H., Macko, S.A. (Eds.), Organic Geochemistry. Plenum Press, New York, pp. 511–533.
Pan, C., Geng, A., Zhong, N., Liu, J., 2010. Kerogen pyrolysis in the presence and absence of water and minerals: Steranes and triterpenoids. Fuel 89, 336–345.
Pancost, R.D., Baas, M., van Geel, B., Sinninghe Damsté, J.S., 2002. Biomarkers as proxies for plant inputs to peats: an example from a sub-boreal ombrotrophic bog. Org. Geochem. 33, 675–690.
Peters, K.E., Moldowan, J.M., 2017. In: Sorkhabia, R. (Ed.), Biomarkers: assessment of source rock thermal maturity. Encyclopedia of Petroleum Geoscience.
Peters, K.E., Walters, C.C., Moldowan, J.M., 2005a. The Biomarker Guide, Volume 1: Biomarkers and Isotopes in the Environment and Human History, 2 edition. Cambridge University Press, Cambridge.
Peters, K.E., Walters, C.C., Moldowan, J.M., 2005b. The Biomarker Guide, Volume 2: Biomarkers and Isotopes in Petroleum Systems and Earth History, 2 edition. Cambridge University Press, Cambridge.
Poprawa, P., Grabowski, J., Grotek, I., 2002. Thermal and burial history of the sub-Tatric nappes and the Podhale basin – constraints from preliminary maturity analysis and modeling. In: Geologica Carpathica 53 (special issue), Proceedings of XVII Congres of CBGA, (Bratislava).
Rieley, G., Collier, R.J., Jones, D.M., Eglinton, G., 1991. The biogeochemistry of Ellesmere Lake, UK - I: source correlation of leaf wax inputs to the sedimentary lipid record. Org. Geochem. 17, 901–912.
Rubinstein, I., Strausz, O.P., Spyckerelle, C., Crawford, R.J., Westlake, D.W.S., 1977. The origin of oil sand bitumens of Alberta. Geochim. Cosmochim. Acta 41, 1341–1353.
Scalan, R.S., Smith, J.E., 1970. An improved measure of the odd-even predominance in the normal alkanes of sediment extracts and petroleum. Geochimica et Cosmocimica Acta 34, 611–620.
Schefuss, E., Ratmeyer, V., Stuut, J.B.W., Jansen, J.H.F., Sinninghe Damstè, J.S., 2003. Carbon isotope analyses of *n*-alkanes in dust from the lower atmosphere over the central eastern Atlantic. Geochim. Cosmochim. Acta 67, 1757–1767.
Seifert, W.K., Moldowan, J.M., 1986. In: Johns, R.B. (Ed.), Use of Biological Markers in Petroleum Exploration. 24. Methods in Geochemistry and Geophysics Book Series, Amsterdam, pp. 261–290.
Sinninghe Damstè, J.S., van Duin, A.C.T., Hollander, D., Kohnen, M.E.L., de Leeuw, J.W., 1995. Early diagenesis of bacteriohopanepolyol derivatives: formation of fossil homohopanoids. Geochim. Cosmochim. Acta 59, 5141–5155.
Sotak, J., 1998a. Sequence stratigraphy approach to the Central Carpathian Paleogene (Eastern Slovakia): eustasy and tectonics as controls of deep sea fan deposition. Slovak Geological Magazine 4, 185–190.
Sotak, J., 1998b. Central Carpathian Paleogene and its constraints. Slovak Geological Magazine 4, 203–211.
Środoń, J., Kotarba, M., Biroń, A., Such, P., Clauer, N., Wojtowicz, A., 2006. Diagenetic history opf the Podhale-Orava Basin and the underlying Tatra sedimentary structural units (Western Carpathians): evidence from XRD and K-Ar of illite-smectite. Clay Miner. 41, 751–774.
Stefanova, M., Oros, D.R., Otto, A., Simoneit, B.R.T., 2002. Polar aromatic biomarkers in the Miocene Maritza-East lignite, Bulgaria. Org. Geochem. 33, 1079–1091.
Świerczewska, A., 2005. The interplay of the thermal and structural histories of the Magura Nappe (Outher Carpathians) in Poland and Slovakia. Mineral. Pol. 36, 91–144.
Ten Haven, H.L., de Leeuw, J.W., Rullkötter, J., Sinninghe Damsté, J.S., 1987. Restricted utility of the pristane/phytane ratio as a palaeoenvironmental indicator. Nature 330, 641–643.
Tissot, B.P., Welte, D.H., 1984. Petroleum Formation and Occurrence, Second ed. Springer, Berlin.
Tokarski, A.K., Świerczewska, A., Zuchiewicz, W., Starek, D., Fodor, L., 2012. Quaternary exhumation of the Carpathians: a record from the Orava-Nowy Targ Intramontane Basin, Western Carpathians (Poland and Slovakia). Geol. Carpath. 63, 257–266.
Tuo, J., Philp, R.P., 2005. Saturated and aromatic diterpenoids and triterpenoids in Eocene coals and mudstones from China. Appl. Geochem. 20, 367–381.
Vanko, J., 1988. A rectified map of recent vertical surface movements in the West Carpathians in Slovakia. J. Geodyn. 10, 147–155.

Volkman, J.K., Maxwell, J.R., 1986. Acyclic isoprenoids as biological markers. In: Johns, R.B. (Ed.), Biological Markers in the Sedimentary Record. Elsevier, Amsterdam, pp. 1–46.
Wagner, M., 2011. Petrologic studies and diagenetic history of coaly matter in the Podhale flysch sediments, southern Poland. Ann. Soc. Geol. Pol. 81, 173–183.
Wakeham, S.G., Schaffner, C., Giger, W., 1979. Polycyclic aromatic hydrocarbons in recent lake sediments – II. Compounds derived from biogenic precursors during early diagenesis. Geochimica et. Cosmochimica Acta 44, 415–429.
Waliczek, M., Solecki, M., 2014. New data on burial and exhumation within Orava-Nowy Targ Intramontane Basin (Western Carpathians): results of vitrinite reflectance studies. XVth International Conference of Young Geologists Her'lany 2014: Międzybrodzie Żywieckie, Poland.
Wang, Y., Fang, X., Zhang, T., Li, Y., Wu, Y., He, D., Wang, Y., 2010. Predominance of even carbon-numberen *n*-alkanes from lacustrine sediments in Linxia Basin, NE Tibetian Plateau: implication for climate change. Appl. Geochem. 25, 1478–1486.
Watycha, L., 1976. The Neogene of the Orava-Nowy Targ Basin (in Polish with English summary). Kwartalnik Geol. 20, 575–585.
Wysocka, A., Łoziński, M., Śmigielski, M., Czarniecka, U., Bojanowski, M., 2018. New data on the age of the sedimentary infill of the Orava-Nowy Targ Basin – a case study of the Bystry Stream succession (Middle/Late Miocene, Western Carpathians). Geological Quarterly 62, 327–343.
Zhang, Z., Zhao, M., Eglinton, G., Lu, H., Huang, C.Y., 2006. Leaf wax lipids as paleovegetational and paleoenvironmental proxies for the Chinese Loess Plateau over the last 170 kyr. Quarternary Science Review 25, 575–594.